Australian Government
Department of Defence
Defence Science and
Technology Organisation

Tracking Anti-Ship Missiles Using Radar and Infra-Red Search and Track: Track Error Performance

Hwa-Tung Ong

Information Integration Branch
Defence Science and Technology Organisation

DSTO–TR–1863

ABSTRACT

The problem of association and fusion of radar and infra-red search and track (IRST) sensor reports is not straightforward, especially because IRST provides only angular measurements while radar provides range and range-rate measurements in addition to azimuth and elevation measurements. In this report, simulation results show that a centralised extended Kalman filter tracker is a solution that can capitalise on the higher angular accuracy of the IRST sensor to provide improved track accuracy performance.

Published by

Defence Science and Technology Organisation
PO Box 1500
Edinburgh, South Australia 5111, Australia

Telephone: (08) 8259 5555
Facsimile: (08) 8259 6567

AR No. 013-655
June, 2006

APPROVED FOR PUBLIC RELEASE

Tracking Anti-Ship Missiles Using Radar and Infra-Red Search and Track: Track Error Performance

EXECUTIVE SUMMARY

Modern anti-ship missiles represent a serious threat to maritime assets. They are designed to fly close to the sea surface and can perform high-acceleration terminal manoeuvres, making them difficult to detect and track in time for effective engagement by shipboard weapons systems.

Following two decades of research and development in ship self defence systems, one of the promising aspects that has emerged is the combination of radar and infra-red search and track (IRST) sensors to improve the detection and tracking of anti-ship missiles.

This is recognised in Project SEA 1448, which is required to deliver enhanced ship self defence against modern anti-ship missiles for the Royal Australian Navy's ANZAC frigates. As part of this project, IRST sensors will be integrated into an upgraded combat system.

In practice, implementation of effective operational data fusion systems is far from simple and fusion of sensor data may actually produce worse results.

In this report, Monte Carlo simulations are employed to quantify the track error achievable using standard tracking algorithms (namely, global nearest neighbour data association and an extended Kalman filter) with and without IRST when tracking non-manoeuvring and manoeuvring missile targets. The aim is to determine whether combining radar with IRST provides significant benefits in reducing track error.

Three missile trajectories are considered:

Straight The missile flies in a straight line at constant speed and height towards the ship.

Weave The missile flies in a sinusoidal line at constant height towards the ship.

Dive The missile flies in a straight line towards the ship and then rapidly climbs to a new height in preparation for a dive attack.

Track error performance is measured in terms of 90% azimuth, elevation and range error levels from 100 Monte Carlo simulation runs for each of the three missile trajectories.

The simulation results confirm that the incorporation of IRST can lead to improved track accuracy performance. The track azimuth and elevation errors drop to the IRST measurement error level, while the track range error does not change significantly. This is to be expected since IRST measures azimuth and elevation but not range.

Contents

Appendices

1 Introduction

Modern anti-ship missiles represent a serious threat to maritime assets. They are designed to fly close to the sea surface and can perform high-acceleration terminal manoeuvres, making them difficult to detect and track in time for effective engagement by shipboard weapons systems.

Following two decades of research and development in ship self defence systems, one of the promising aspects that has emerged is the combination of radar and infra-red search and track (IRST) sensors to improve the detection and tracking of anti-ship missiles.

This is recognised in Project SEA 1448, which is required to deliver enhanced ship self defence against modern anti-ship missiles for the Royal Australian Navy's ANZAC frigates. As part of this project, IRST sensors will be integrated into an upgraded combat system.

Some of the benefits of combining radar with IRST are [Missirian & Ducruet 1997, Misanin 1995]

Increased detection performance Radar performance is degraded at low elevations due to surface clutter, multipath propagation and unfavourable evaporative ducting conditions. IRST operates at different frequency bands and provides additional means of target detection via aerodynamic skin heating and engine exhaust plumes.

Reduced threat alert time For an incoming missile, skimming along the surface of the sea, the time between when the missile becomes visible on the radar horizon and when it reaches its target is very short. The time can be less than 30 seconds for some types of anti-ship missile [Horman, Stapleton, Hepfer, Headley & Stapleton 1996]. An IRST, performing dedicated horizon search, can provide earlier target detection and cue a radar to the target for more observations.

Reduced vulnerability to ECM Radar emissions are restricted when covertness is required, or to minimise susceptibility to jamming. In such circumstances, an IRST may become the primary sensor to guard against anti-ship missiles.

Another potential benefit of combining radar and IRST sensors is improved track accuracy which is important for sensor cueing and weapons control functions. By appropriate means of multisensor data fusion, the radar's accurate range measurements (but not-so-accurate angle measurements) can be combined with the IRST's accurate angle measurements to provide a fused estimate of the target's location that is of reduced error [Hall & Llinas 1997].

In practice, implementation of effective operational data fusion systems is far from simple and fusion of sensor data may actually produce worse results [Hall & Llinas 1997].

Other authors have reported track error performance using IRST alone [Maltese 2001], enhanced angular track accuracy achievable by fusing IRST and ESM sensors [Maltese & Lucas 2000], the effect of the choice of coordinate system on track error performance of radar and IRST fusion [Simard & Bégin 1993], and significant reduction in track error by applying Multiple Hypothesis Tracking/Interacting Multiple Models (MHT/IMM) on

radar and IRST data [Blackman, Dempster & Roszkowski 1997, Dempster, Blackman, Roszkowski & Sasaki 1998].

In this report, Monte Carlo simulations are employed to quantify the track error achievable using standard tracking algorithms with and without IRST when tracking non-manoeuvring and manoeuvring missile targets. The aim is to determine whether combining radar with IRST provides significant benefits in reducing track error.

Only generic radar and IRST sensor models are used and no attempt has been made to model environmental conditions. Simulated anti-ship missile trajectories include weave and dive. Further details of the simulated missile trajectories, sensor models and tracking algorithms are given in Sections 2, 3 and 4 respectively. The error performance statistic is defined in Section 5. The simulation results are given and discussed in Section 6. Section 7 provides the conclusions.

2 Missile Trajectories

Three possible missile trajectories are considered:

Straight The missile flies in a straight line at constant speed and height towards the ship.

Weave The missile flies in a sinusoidal line at constant height towards the ship.

Dive The missile flies in a straight line towards the ship and then rapidly climbs to a new height in preparation for a dive attack.

The ship is located at the origin. Each of the simulated trajectories lasts for 27 seconds. Specific details are given in the subsections that now follow.

2.1 Straight

Specific parameters, relative to the ship origin, are:

Bearing 90°

Start Range 19 km

Speed 700 m/s

Height 10 m

2.2 Weave

Specific parameters, relative to the ship origin, are:

Bearing 0°

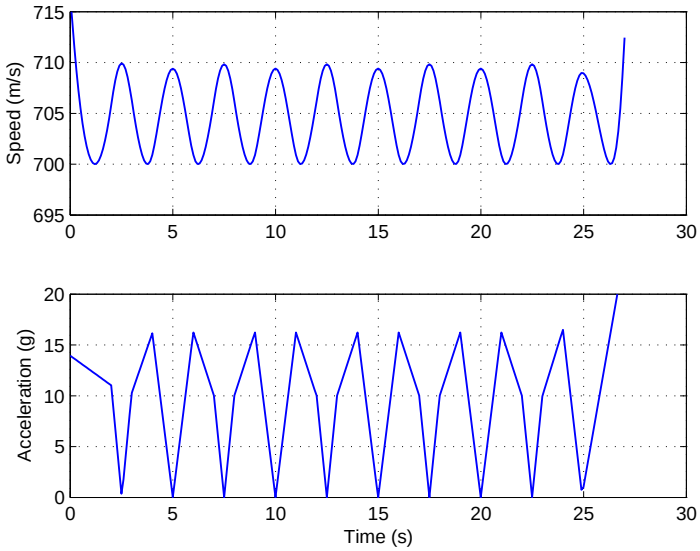

Figure 1: *Weave missile speed and acceleration*

Start Range 19 km

Height 10 m

Weave Period 5 s

Weave Amplitude 89 m

Figure 1 gives the instantaneous speed and acceleration of the weave missile. It can be seen that acceleration reaches just above 15 g (where 1 g equals 9.81 m/s^2).

2.3 Dive

The dive trajectory is based on the bunt manoeuvre scenario of Maltese (2001). Figure 2 gives the trajectory simulated for 27 seconds only. Most of the dive portion occurs after 27 seconds and is therefore not apparent in the figure. Figure 3 gives the instantaneous speed and acceleration of the dive missile. It can be seen that acceleration can exceed 20 g during the height increase and 30 g as the missile dives.

3 Sensor Models

The radar and IRST sensor are characterised by range-dependent "probability of target detection" curves for a constant probability of false alarm. Measurement accuracy is modelled by the Gaussian distribution for the sensor noise. Both sensors rotate 360° and have the scan times as given in Table 1. Note that two surveillance configurations are modelled, radar-only and radar-plus-IRST configurations.

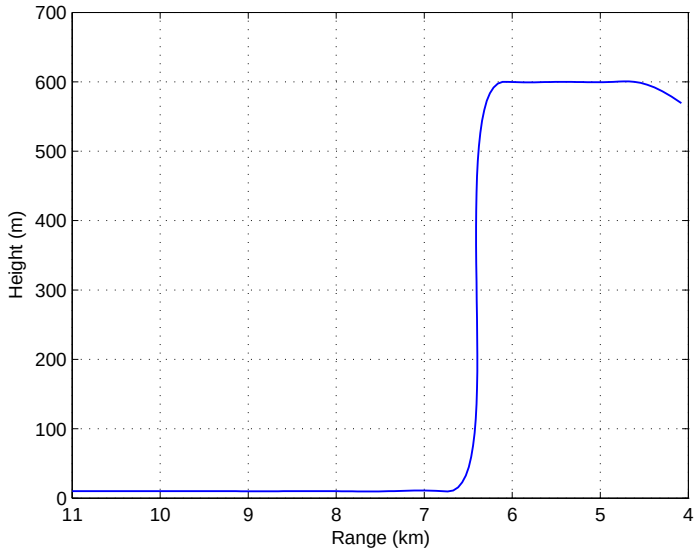

Figure 2: *Dive trajectory*

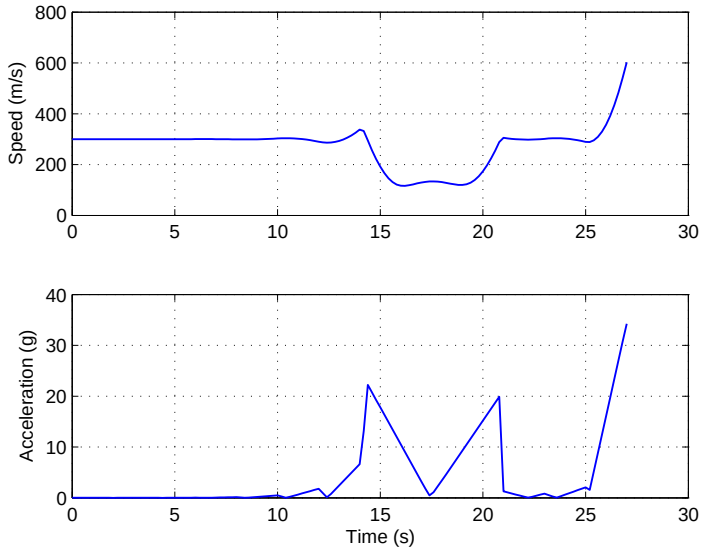

Figure 3: *Dive missile speed and acceleration*

Table 1: *Sensor scan times*

Configuration	Radar	IRST
Radar-only	5 s	-
Radar-plus-IRST	5 s	1 s

Table 2: *Radar measurement accuracy*

Measurement	Error standard deviation
Range	60 m
Azimuth	0.5°
Elevation	1°
Range-rate	0.7 m/s

Table 3: *Radar field of view*

Azimuth	360°
Elevation	0°–30°
Range	1–450 km
Range-rate	0–1000 m/s

The sensors are ideal in that they have negligible registration error and they resolve targets fully.

Note that environmental effects such as clutter, multipath propagation and evaporative ducts are not modelled. These effects could degrade sensor detection performance in practice and reduce tracking performance as a result. Future work could look at the impact of these effects on tracking performance.

3.1 Radar

For rapidly-approaching targets, it is assumed that the signal-to-noise ratio (SNR) for targets is not attenuated by the radar processor's Doppler notch.

For a 10^{-5} probability of false alarm, the probability of detection is 1.0 for a Swerling 1 target at ranges less than 19 km, according to textbook formulae [Blackman & Popoli 1999, sec. 2.2].

If the radar detects a target, it returns noisy measurements of the azimuth, elevation, range and range-rate of the target. Table 2 gives the standard deviations chosen for the measurement noise. False alarm measurements are uniformly distributed over the radar field of view. The radar field of view is given in Table 3.

3.2 IRST

The IRST sensor is an array of 640 by 512 detector elements which captures the infrared scene once every 1.5 ms. For a target at range R, the IRST measures a signal with amplitude that is proportional to R^{-2} [Blackman & Popoli 1999, sec. 2.3.7]. This signal is corrupted by Gaussian noise. A threshold is set to maintain a false alarm rate of not more than 1.0 per hour over the entire array of detector elements. Given this threshold, the signal strength from the target is such that, at $R = 11$ km, the probability of detection

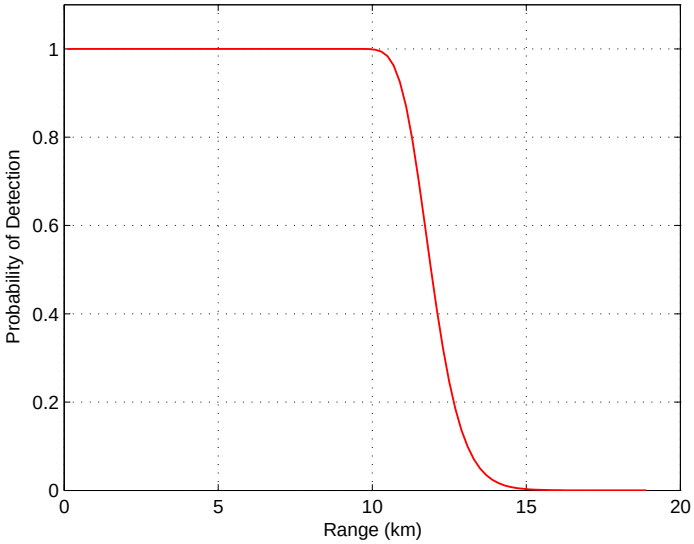

Figure 4: *The probability of target detection in every scan of the IRST*

Table 4: *IRST measurement accuracy*

Measurement	Error standard deviation
Azimuth	0.5 mrad
Elevation	0.5 mrad

is 0.9. Figure 4 depicts the resulting single-scan target detection probability curve for the IRST.

If a target is detected, the IRST measures the azimuth and elevation of the target. Table 4 gives the values chosen for the IRST measurement noise standard deviations. For a false alarm, the measured azimuth and elevation are uniformly distributed over the IRST field of view. The IRST field of view is given in Table 5.

Table 5: *IRST field of view*

Azimuth	360°
Elevation	0°–10°
Range	0.1–30 km

4 Target Tracking

Target tracking is performed in rectangular coordinates. The track state is composed of position and velocity estimates of the target.

$$\mathbf{x} = \begin{bmatrix} x \\ y \\ z \\ \dot{x} \\ \dot{y} \\ \dot{z} \end{bmatrix} \tag{1}$$

Reports from radar and IRST sensors are sent directly to a central tracker that is based on the Extended Kalman Filter (EKF).

The tracker comprises the following processes:

- Data association
- Track initiation
- Track update
- Track deletion

Details of these are given below.

4.1 Data Association

Before a track can be updated by a report, the report must first be associated with the track. This process generally involves calculating a correlation statistic for each track-report pair and assigning reports to tracks based on these correlation statistics.

The gating of reports also forms part of the process. Gating is applied to determine which reports are reports of new targets, i.e., targets which have not been detected previously. For reports of new targets, new tracks are created through the process of track initiation.

A basic assignment method is the Global Nearest Neighbour (GNN) method which considers optimal assignment of reports to tracks in a fixed frame of time. A more sophisticated method is the Multiple Hypothesis Tracking (MHT) method which considers optimal assignment over multiple frames of time. MHT is computationally intensive but is useful for tracking closely-spaced targets. This is where single-frame methods have difficulty making correct assignments. Further details of these methods can be found in standard textbooks.

In this report, the tracker applies GNN logic with a frame time of 0.5 seconds. MHT was not considered to be necessary for the single target scenarios of interest.

The correlation statistic for a track with state $\mathbf{x}$ and covariance $\mathbf{P}$, and a report with measurement $\mathbf{z}$ and measurement covariance $\mathbf{R}$ is given by

$$G - (\mathbf{z} - \mathbf{h}(\mathbf{x}))'(\mathbf{HPH}' + \mathbf{R})^{-1}(\mathbf{z} - \mathbf{h}(\mathbf{x})) \tag{2}$$

where $\mathbf{h}$ is the measurement function, $\mathbf{H}$ is the Jacobian of the measurement function, and G is the gating threshold. Note that the track state and covariance are quantities predicted from the time of the most recent track update to the time of the report being correlated. More details are given in Section 4.3 on the track update process.

The gating threshold G is an adjustable parameter that discriminates reports of new targets from those of existing targets. It is set to 10^5 in the EKF tracker for gating both radar or IRST reports.

The Auction algorithm is used to assign the reports to tracks. This algorithm is described in Section 6.5.1 of Blackman & Popoli.

4.2 Track Initiation

Each report that is not associated with a track after the data association process is converted from spherical to rectangular coordinates to provide the initial track position and track position covariance. To minimise the biases introduced by the conversion, the formulae in Appendix A are applied.

For IRST reports, range is not measured. In this case, the conversion assumes a 'measured' range of 50 km with a 'measurement error' standard deviation of 50 km. (As suggested by the referee of this report, an initial range of 30 km might be a more appropriate assumption given that the IRST field of view for range is 0–30 km.)

The initial track velocity is set to zero and the initial track velocity standard deviation is set to 267 m/s in each coordinate.

To incorporate the range-rate measurement in radar reports, a single EKF update is performed. The steps are given in Table 6.

The initial track state and covariance represent a **tentative track** which would not be output to an operator display process because it may be a false track. Displaying such tentative tracks would lead to an unacceptably high number of false tracks. This is especially true in heavy clutter environments where there are many spurious reports.

The track becomes an **established track** after it is updated by two more correlated reports. This track is then 'safe' to output because it is more likely to represent a target of interest than to be a false track.

4.3 Track Update

When an existing track is associated with a report by the data association process, it is updated via a two-step procedure. The first step of this procedure is to *predict* the track to the time of the report. The second step is to *correct* the predicted track using the measured data.

Table 6: *Steps to incorporate a range-rate measurement into the initial track state and covariance*

Compute Jacobian matrix

$$\mathbf{H} = \begin{bmatrix} (\dot{x} - \dot{r}x/r)/r & (\dot{y} - \dot{r}y/r)/r & (\dot{z} - \dot{r}z/r)/r & x/r & y/r & z/r \end{bmatrix} \quad (3)$$

where (x, y, z) and $(\dot{x}, \dot{y}, \dot{z})$ are the initial track state position and velocity before the range-rate update, and

$$r = \sqrt{x^2 + y^2 + z^2} \quad (4)$$

$$\dot{r} = (x\dot{x} + y\dot{y} + z\dot{z})/r \quad (5)$$

Compute Kalman gain

$$\mathbf{K} = \mathbf{P}\mathbf{H}'(\mathbf{H}\mathbf{P}\mathbf{H}' + \sigma_{\dot{r}}^2)^{-1} \quad (6)$$

where $\mathbf{P}$ is the initial track covariance before the range-rate update, and $\sigma_{\dot{r}}$ is the range-rate measurement error standard deviation, assumed to be known.

Update initial track state

$$\mathbf{x} \leftarrow \mathbf{x} + \mathbf{K}(z - \dot{r}) \quad (7)$$

where z is the range-rate measurement.

Update initial track covariance

$$\mathbf{P} \leftarrow \mathbf{P} - \mathbf{K}\mathbf{H}\mathbf{P} \quad (8)$$

The update procedure for the EKF tracker is given in Table 7. This procedure assumes a white noise constant velocity target [Blackman & Popoli 1999, sec. 4.2.2]. For radar reports, it converts the measured range, azimuth and elevation to rectangular coordinates using the formulae in Appendix A. For IRST reports, the update procedure is given in Table 8.

Note that the process noise parameter q (in (11) of Table 7) is set empirically to obtain some ability for the EKF tracker to track through target manoeuvres whilst maintaining an acceptable track error performance during the non-manoeuvring sections of target trajectories.

If improved performance on manoeuvring targets is desired, the Interacting Multiple Models (IMM) tracking approach is recommended. This is a standard approach where the target motion is modelled as a stochastic process that can switch between several different dynamic models. For example, a target moving at constant velocity for a period of time and then switching to constant acceleration motion can be modelled. An IMM tracker can provide improved track accuracy performance at increased computational cost compared with an EKF tracker.

4.4 Track Deletion

Tracks are deleted if they have not been updated for more than 10 seconds, or if the predicted track error variance (from the diagonal of the track covariance matrix $\mathbf{P}$) exceeds 10^5 m^2 in the x or y coordinate, or 5000 m^2 in the z coordinate. Under these conditions, tracks are said to be lost or to have 'gone stale'.

5 Performance Measure

In this report, track error performance is measured in terms of 90% azimuth, elevation and range error levels from 100 Monte Carlo simulation runs for each of the scenario described in Section 2.

For each Monte Carlo simulation run, the track azimuth/elevation/range error (i.e., absolute difference between the track and true values) is computed and sampled at every 0.2 seconds. If there are multiple tracks at a given sample time, the smallest track error at that time is taken. If no track exists at a given sample time, no error sample is taken.

Error samples collected at each time point are sorted in ascending order. The 90% error level bounds 90% of the error samples. It is taken as the Mth sorted error sample, where $M = \lfloor 0.9(N+1) \rfloor$ and N denotes the number of samples.

6 Results and Discussion

Figures 5, 6 and 7 show the track azimuth, elevation and range errors for straight, weave and dive missile trajectories respectively. Also shown are the radar and IRST

Table 7: *EKF track update procedure*

Predict

$$\mathbf{x} \leftarrow \mathbf{F}\mathbf{x} \tag{9}$$

$$\mathbf{P} \leftarrow \mathbf{F}\mathbf{P}\mathbf{F}' + \mathbf{Q} \tag{10}$$

where

$$\mathbf{F} = \begin{bmatrix} \mathbf{I}_3 & T\mathbf{I}_3 \\ \mathbf{0}_3 & \mathbf{I}_3 \end{bmatrix}, \quad \mathbf{Q} = \begin{bmatrix} \frac{T^3}{3}\mathbf{I}_3 & \frac{T^2}{2}\mathbf{I}_3 \\ \frac{T^2}{2}\mathbf{I}_3 & T\mathbf{I}_3 \end{bmatrix} q \tag{11}$$

where $q = 100$, and T is the time increment to predict the track to the time of the report. $\mathbf{I}_3$ denotes a 3-by-3 identity matrix, and $\mathbf{0}_3$ denotes a 3-by-3 zero matrix.

Correct For radar reports which have range, azimuth, elevation and range-rate measurements:

Compute Jacobian matrix

$$\mathbf{H} = \begin{bmatrix} 1 & 0 & 0 & 0 & 0 & 0 \\ 0 & 1 & 0 & 0 & 0 & 0 \\ 0 & 0 & 1 & 0 & 0 & 0 \\ (\dot{x} - \dot{r}x/r)/r & (\dot{y} - \dot{r}y/r)/r & (\dot{z} - \dot{r}z/r)/r & x/r & y/r & z/r \end{bmatrix} \tag{12}$$

where (x, y, z) and $(\dot{x}, \dot{y}, \dot{z})$ are the predicted track state position and velocity, and

$$r = \sqrt{x^2 + y^2 + z^2} \tag{13}$$

$$\dot{r} = (x\dot{x} + y\dot{y} + z\dot{z})/r \tag{14}$$

Compute Kalman gain

$$\mathbf{K} = \mathbf{P}\mathbf{H}'(\mathbf{H}\mathbf{P}\mathbf{H}' + \mathbf{R})^{-1} \tag{15}$$

where $\mathbf{P}$ is the predicted track covariance, and $\mathbf{R}$ is the measurement covariance.

Update predicted track state

$$\mathbf{x} \leftarrow \mathbf{x} + \mathbf{K}(\mathbf{z} - [x\, y\, z\, \dot{r}]') \tag{16}$$

where $\mathbf{z}$ is the measurement vector comprising of the 3D position and measured range-rate. The 3D position is in rectangular coordinates and is obtained by converting the spherical measurements (of range, azimuth and elevation) using formulae in Appendix A.

Update predicted track covariance

$$\mathbf{P} \leftarrow \mathbf{P} - \mathbf{K}\mathbf{H}\mathbf{P} \tag{17}$$

Table 8: *EKF track update procedure for IRST reports*

Predict the track as in Table 7 and then correct the predicted track as follows:

Compute Jacobian matrix

$$\mathbf{H} = \begin{bmatrix} -y/r_g^2 & x/r_g^2 & 0 & 0 & 0 & 0 \\ xc & yc & r_g/r^2 & 0 & 0 & 0 \end{bmatrix} \tag{18}$$

where (x, y, z) is the predicted track state position, and

$$r_g = \sqrt{x^2 + y^2} \tag{19}$$

$$r = \sqrt{x^2 + y^2 + z^2} \tag{20}$$

$$c = -z/(r^2 r_g) \tag{21}$$

Compute Kalman gain

$$\mathbf{K} = \mathbf{P}\mathbf{H}' \left(\mathbf{H}\mathbf{P}\mathbf{H}' + \begin{bmatrix} \sigma_a^2 & 0 \\ 0 & \sigma_e^2 \end{bmatrix} \right)^{-1} \tag{22}$$

where $\mathbf{P}$ is the predicted track covariance, and σ_a and σ_e are azimuth and elevation measurement error standard deviations, assumed to be known.

Update predicted track state

$$\mathbf{x} \leftarrow \mathbf{x} + \mathbf{K} \begin{bmatrix} \hat{a} - \tan^{-1}(y, x) \\ \hat{e} - \tan^{-1}(z, r_g) \end{bmatrix} \tag{23}$$

where $\hat{a}$ and $\hat{e}$ are the measured azimuth and elevation. Note that if $|\hat{a} - \tan^{-1}(y, x)| > \pi$, the appropriate multiple of 2π should be added or subtracted from $\hat{a} - \tan^{-1}(y, x)$ to obtain a value between $-\pi$ and π to replace it in the above equation.

Update predicted track covariance

$$\mathbf{P} \leftarrow \mathbf{P} - \mathbf{K}\mathbf{H}\mathbf{P} \tag{24}$$

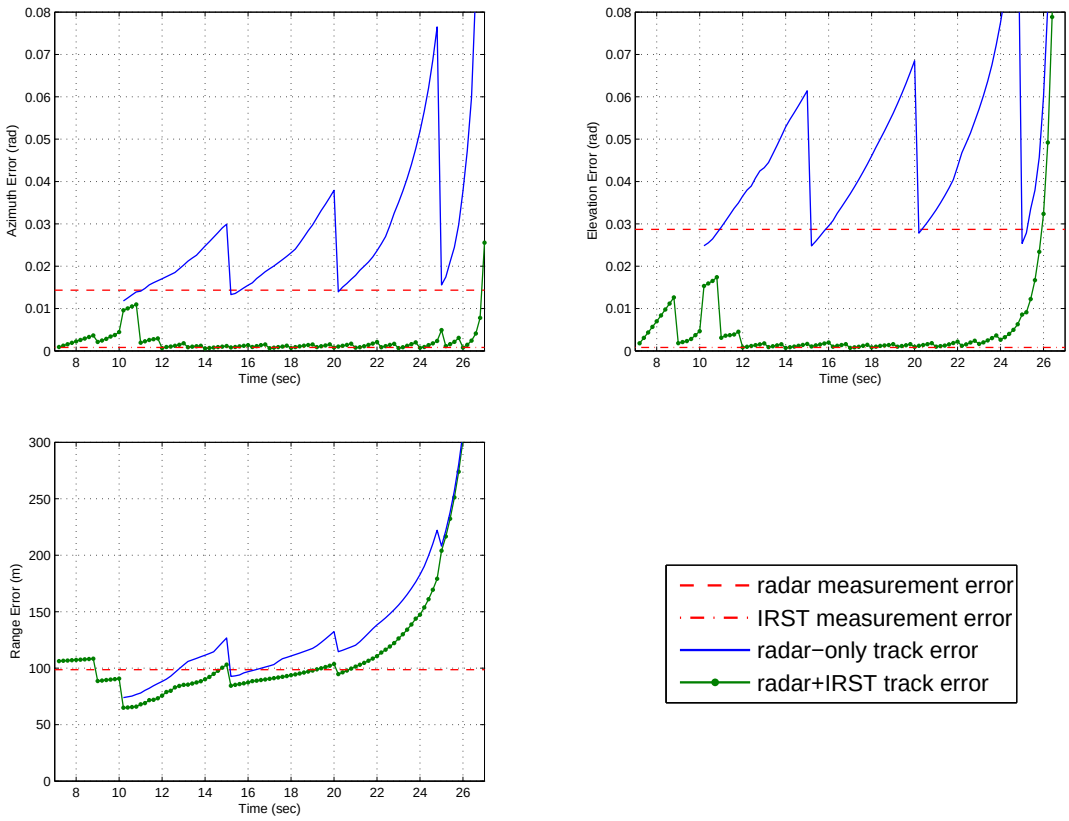

Figure 5: *Track error for the straight missile trajectory*

measurement errors for comparison. These errors correspond to the 90% quantile of the absolute error distribution assuming a Gaussian distribution for the sensor error with the standard deviations given in Table 2 and Table 4.

The results confirm that the incorporation of IRST can lead to improved track accuracy performance. The track azimuth and elevation errors drop to the IRST measurement error level, while the track range error does not change significantly. This is to be expected since IRST measures azimuth and elevation but not range.

Although not the focus of this report, the results also indicate earlier track initiation due to the faster scan rate of the IRST sensor. This is apparent in the figures. The accuracy performance for radar+IRST tracks is available after at most 7 seconds into the simulation compared with 10–11 seconds for radar-only tracks.

6.1 Straight

The results in Figure 5 demonstrate the value of sensor fusion. Track angle errors are reduced to the level of that of the more accurate IRST sensor, while track range error is almost unchanged.

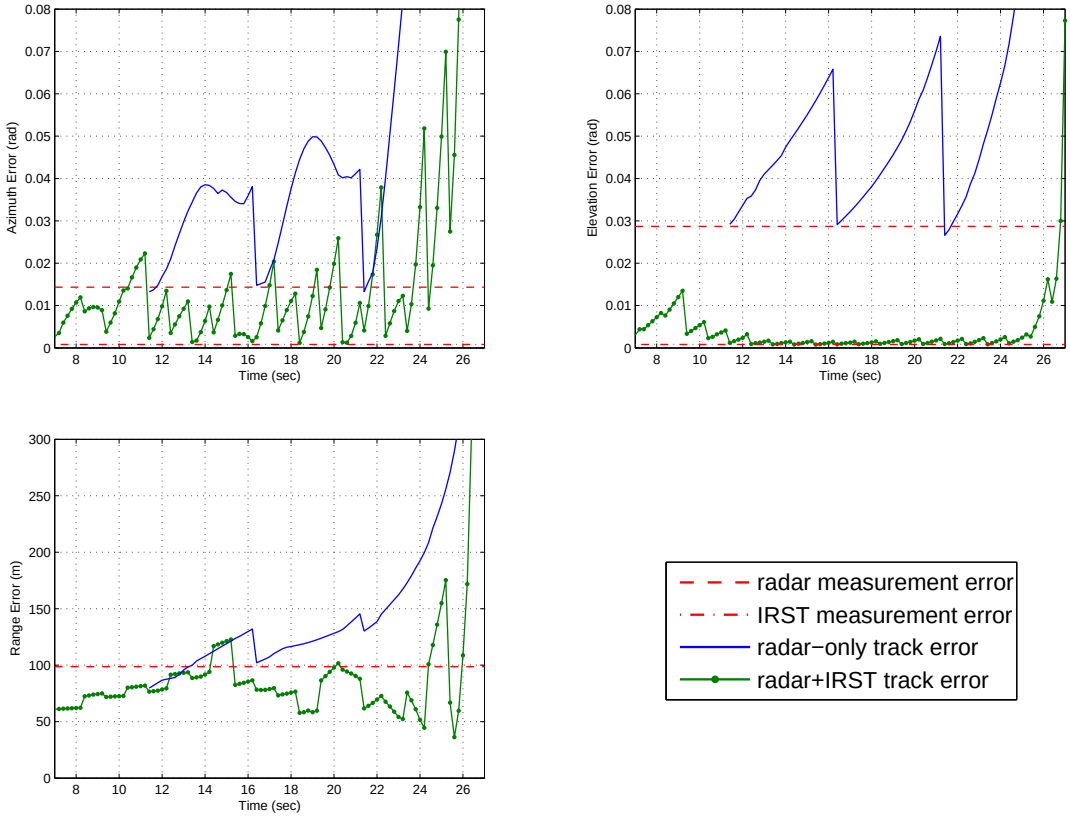

Figure 6: *Track error for the weave missile trajectory*

6.2 Weave

For a weaving missile that is manoeuvring predominantly in the azimuth axis, it can be seen that the track error along this axis is elevated compared with the performance for the straight trajectory. There is some slight effect of the weaving on radar+IRST track range error which is noticeable in Figure 6.

6.3 Dive

In the case of the dive trajectory where the missile executes rapid changes in elevation, the increased scan rate of the IRST sensor helps the EKF tracker maintain track on the target and keep the track elevation accuracy close to the accuracy of the IRST measurement.

Curiously, the results for the dive trajectory do not exhibit the same behaviour compared with the results for the straight and weaving trajectories near the end of the simulation. That is, the track errors for the dive trajectory do not shoot off the graph after 27 seconds. The reason for this is that the missile is still about 4 km away from the sensors in this scenario. In the straight and weaving missile scenarios, the missile is only a hundred metres or so away after 27 seconds have elapsed. At such a close range, the EKF tracker

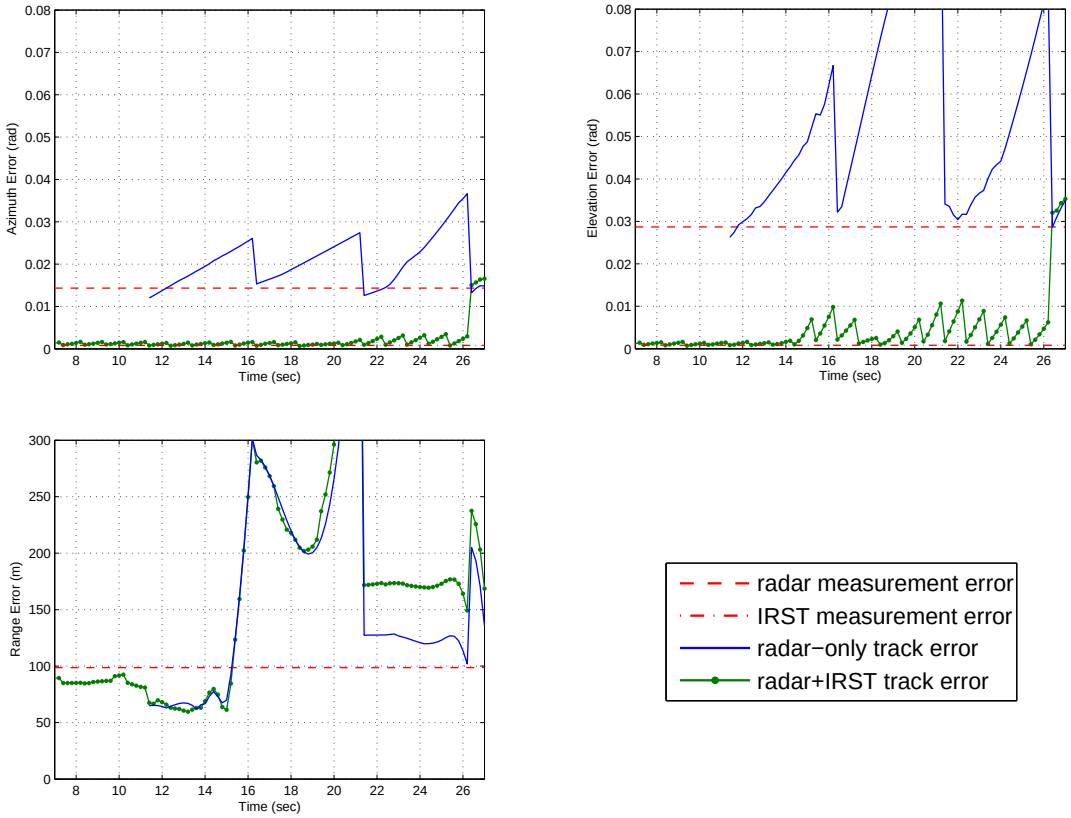

Figure 7: *Track error for the dive missile trajectory*

cannot cope with the nonlinearity of the measurements.

In practice, targets at very close range may be detected in more than one sensor resolution cell and sensor reports may become unreliable or unavailable. It is hoped, of course, that a missile never gets within 4 km of the ship!

7 Conclusions

The problem of association and fusion of radar and IRST sensor reports is not straightforward, especially because IRST provides only angular measurements while radar provides range and range-rate measurements as well. In this report, simulation results have shown that a centralised EKF tracker is a solution that can capitalise on the higher angular accuracy of the IRST sensor to provide improved track accuracy performance.

References

Blackman, S. & Popoli, R. (1999) *Design and Analysis of Modern Tracking Systems*, Artech House.

Blackman, S. S., Dempster, R. J. & Roszkowski, S. H. (1997) IMM/MHT applications to radar and IR multitarget tracking, *in Signal and Data Processing of Small Targets 1997*, Vol. 3163, pp. 429–439.

Dempster, R. J., Blackman, S. S., Roszkowski, S. H. & Sasaki, D. M. (1998) IMM/MHT solution to radar and multisensor benchmark tracking problems, *in Signal and Data Processing of Small Targets 1998*, Vol. 3373, pp. 331–342.

Hall, D. L. & Llinas, J. (1997) An introduction to multisensor data fusion, *Proceedings of the IEEE* **85**(1), 6–23.

Horman, S. R., Stapleton, R. A., Hepfer, K. C., Headley, R. M. & Stapleton, J. K. (1996) Interacting integration of passive infrared and radar horizon surveillance sensors to extend acquisition and firm track ranges, *in AGARD Proceedings of Multi-Sensor Multi-Target Data Fusion, Tracking and Identification Techniques for Guidance and Control Applications*, Vol. AGARD-AG-337, pp. 14–31.

Maltese, D. (2001) Naval aid defense: multiple model approach to the angular tracking and targeting of anti-ship missiles, *in Signal Processing, Sensor Fusion, and Target Recognition X*, Vol. 4380 of *Proc. SPIE*, pp. 63–74.

Maltese, D. & Lucas, A. (2000) IRST-ESM data fusion: a full silent search function in naval air defense, *in Signal Processing, Sensor Fusion, and Target Recognition IX*, Vol. 4052 of *Proc. SPIE*, pp. 229–239.

Misanin, J. E. (1995) Shipboard infrared search and track cost and operational effectiveness analysis, *in Infrared Technology XXI*, Vol. 2552 of *Proc. SPIE*, pp. 214–223.

Missirian, J.-M. & Ducruet, L. (1997) IRST: a key system in modern warfare, *in Infrared Technology and Applications XXIII*, Vol. 3061 of *Proc. SPIE*, pp. 554–565.

Simard, M.-A. & Bégin, F. (1993) Central level fusion of radar and IRST contacts and the choice of coordinate system, *in Signal and Data Processing of Small Targets 1993*, Vol. 1954 of *Proc. SPIE*, pp. 462–472.

Suchomski, P. (1999) Explicit expressions for debiased statistics of 3D converted measurements, *IEEE Transactions on Aerospace and Electronic Systems* **35**(1), 368–370.

Appendix A Formulae for Converting Measurements From Spherical to Rectangular Coordinates

The formulae are due to Suchomski [1999]. Denote range, azimuth and elevation measurements by r, a and e respectively. Denote measurement error standard deviation by σ_r, σ_a and σ_e. Then the converted measurement (x, y, z) and measurement covariance $\mathbf{R}$ are given by:

$$\begin{aligned} x &= r\cos a\cos e[\exp(-\sigma_a^2-\sigma_e^2)-\exp(-\sigma_a^2/2-\sigma_e^2/2)] && \text{(A1)}\\ y &= r\sin a\cos e[\exp(-\sigma_a^2-\sigma_e^2)-\exp(-\sigma_a^2/2-\sigma_e^2/2)] && \text{(A2)}\\ z &= r\sin e[\exp(-\sigma_e^2)-\exp(-\sigma_e^2/2)] && \text{(A3)}\\ \mathbf{R} &= \begin{bmatrix} R_{xx} & R_{xy} & R_{xz}\\ R_{xy} & R_{yy} & R_{yz}\\ R_{xz} & R_{yz} & R_{zz}\end{bmatrix} && \text{(A4)}\end{aligned}$$

where

$$\begin{aligned} R_{xx} &= [r^2(\beta_x\beta_{xy}-\alpha_x\alpha_{xy})+\sigma_r^2(2\beta_x\beta_{xy}-\alpha_x\alpha_{xy})]\exp(-2\sigma_a^2-2\sigma_e^2) && \text{(A5)}\\ R_{xy} &= [r^2(\beta_{xy}-\alpha_{xy}\exp\sigma_a^2)+\sigma_r^2(2\beta_{xy}-\alpha_{xy}\exp\sigma_a^2)]\sin a\cos a\exp(-4\sigma_a^2-2\sigma_e^2) && \text{(A6)}\\ R_{xz} &= [r^2(1-\exp\sigma_e^2)+\sigma_r^2(2-\exp\sigma_e^2)]\cos a\sin e\cos e\exp(-\sigma_a^2-4\sigma_e^2) && \text{(A7)}\\ R_{yy} &= [r^2(\beta_y\beta_{xy}-\alpha_y\alpha_{xy})+\sigma_r^2(2\beta_y\beta_{xy}-\alpha_y\alpha_{xy})]\exp(-2\sigma_a^2-2\sigma_e^2) && \text{(A8)}\\ R_{yz} &= [r^2(1-\exp\sigma_e^2)+\sigma_r^2(2-\exp\sigma_e^2)]\sin a\sin e\cos e\exp(-\sigma_a^2-4\sigma_e^2) && \text{(A9)}\\ R_{zz} &= [r^2(\beta_z-\alpha_z)+\sigma_r^2(2\beta_z-\alpha_z)]\exp(-2\sigma_e^2) && \text{(A10)}\end{aligned}$$

where

$$\begin{aligned} \alpha_x &= \sin^2 a\sinh\sigma_a^2+\cos^2 a\cosh\sigma_a^2 && \text{(A11)}\\ \alpha_y &= \sin^2 a\cosh\sigma_a^2+\cos^2 a\sinh\sigma_a^2 && \text{(A12)}\\ \alpha_z &= \sin^2 e\cosh\sigma_e^2+\cos^2 e\sinh\sigma_e^2 && \text{(A13)}\\ \alpha_{xy} &= \sin^2 e\sinh\sigma_e^2+\cos^2 e\cosh\sigma_e^2 && \text{(A14)}\\ \beta_x &= \sin^2 a\sinh(2\sigma_a^2)+\cos^2 a\cosh(2\sigma_a^2) && \text{(A15)}\\ \beta_y &= \sin^2 a\cosh(2\sigma_a^2)+\cos^2 a\sinh(2\sigma_a^2) && \text{(A16)}\\ \beta_z &= \sin^2 e\cosh(2\sigma_e^2)+\cos^2 e\sinh(2\sigma_e^2) && \text{(A17)}\\ \beta_{xy} &= \sin^2 e\sinh(2\sigma_e^2)+\cos^2 e\cosh(2\sigma_e^2) && \text{(A18)}\end{aligned}$$

DISTRIBUTION LIST

Tracking Anti-Ship Missiles Using Radar and Infra-Red Search and Track: Track Error Performance

Hwa-Tung Ong

	Number of Copies
DEFENCE ORGANISATION	
Task Sponsor	
Director General Maritime Development	1 (printed)
S&T Program	
Chief Defence Scientist	1
Deputy Chief Defence Scientist Policy	1
Deputy Chief Defence Scientist Programs	Doc Data Sheet and Exec Summ
Deputy Chief Defence Scientist Information	Doc Data Sheet and Exec Summ
Deputy Chief Defence Scientist Aerospace	Doc Data Sheet and Exec Summ
AS Science Corporate Management	1
Director General Science Policy Development	1
Counsellor, Defence Science, London	Doc Data Sheet
Counsellor, Defence Science, Washington	Doc Data Sheet
Scientific Adviser to MRDC, Thailand	Doc Data Sheet
Scientific Adviser Joint	1
Navy Scientific Adviser	1
Scientific Adviser, Army	Doc Data Sheet and Dist List
Air Force Scientific Adviser	Doc Data Sheet and Exec Summ
Scientific Adviser to the DMO	Doc Data Sheet and Dist List
Chief, Intelligence, Surveillance and Reconnaissance Division	Doc Data Sheet and Dist List
Research Leader, Information Integration	Doc Data Sheet and Dist List
Head, Tracking and Sensor Fusion	1
Dr Branko Ristic, Tracking and Sensor Fusion	1
Dr Martin Oxenham, Tracking and Sensor Fusion	1
Dr Hwa-Tung Ong, Tracking and Sensor Fusion	1
Chief, Maritime Operations Division	Doc Data Sheet and Exec Summ

Dr Patrick Morgan, ANZAC S&T Adviser	Doc Data Sheet and Exec Summ
Dr David Kershaw, AWD S&T Adviser	Doc Data Sheet and Exec Summ
Dr Shane Canney, Head Surface Combatant Combat Systems	Doc Data Sheet and Exec Summ
Dr Leigh Powis, Electronic Warfare and Radar Division	Doc Data Sheet and Exec Summ
Mr Nick Lioutas, Electronic Warfare and Radar Division	1
Mr Peter Sarunic, Electronic Warfare and Radar Division	1
DSTO Library and Archives	
Library Edinburgh	2 (printed)
Defence Archives	1 (printed)
Capability Development Group	
Director General Capability and Plans	Doc Data Sheet
Assistant Secretary Investment Analysis	Doc Data Sheet
Director Capability Plans and Programming	Doc Data Sheet
Director General Australian Defence Simulation Office	Doc Data Sheet
Chief Information Officer Group	
Head Information Capability Management Division	Doc Data Sheet
AS Information Strategy and Futures	Doc Data Sheet
Director General Information Services	Doc Data Sheet
Strategy Group	
Director General Military Strategy	Doc Data Sheet
Assistant Secretary Governance and Counter-Proliferation	Doc Data Sheet
Navy	
Director General Navy Capability, Performance and Plans, Navy Headquarters	Doc Data Sheet
Director General Navy Strategic Policy and Futures, Navy Headquarters	Doc Data Sheet
Deputy Director (Operations) Maritime Operational Analysis Centre, Building 89/90, Garden Island, Sydney Deputy Director (Analysis) Maritime Operational Analysis Centre, Building 89/90, Garden Island, Sydney	Doc Data Sheet and Dist List
Army	
ABCA National Standardisation Officer, Land Warfare Development Sector, Puckapunyal	Doc Data Sheet (pdf format)
SO (Science), Deployable Joint Force Headquarters (DJFHQ)(L), Enoggera QLD	Doc Data Sheet

SO (Science), Land Headquarters (LHQ), Victoria Barracks, NSW	Doc Data Sheet and Exec Summ
Air Force	
SO (Science), Headquarters Air Combat Group, RAAF Base, Williamtown	Doc Data Sheet and Exec Summ
Joint Operations Command	
Director General Joint Operations	Doc Data Sheet
Chief of Staff Headquarters Joint Operation Command	Doc Data Sheet
Commandant, ADF Warfare Centre	Doc Data Sheet
Director General Strategic Logistics	Doc Data Sheet
COS Australian Defence College	Doc Data Sheet
Intelligence and Security Group	
Assistant Secretary, Concepts, Capabilities and Resources	1
DGSTA, DIO	1
Manager, Information Centre, DIO	1
Director Advanced Capabilities, DIGO	Doc Data Sheet
Defence Materiel Organisation	
Deputy CEO, DMO	Doc Data Sheet
Head Aerospace Systems Division	Doc Data Sheet
Head Maritime Systems Division	Doc Data Sheet
Program Manager Air Warfare Destroyer	Doc Data Sheet
CDR Joint Logistics Command	Doc Data Sheet
GWEO-DDP	Doc Data Sheet
UNIVERSITIES AND COLLEGES	
Australian Defence Force Academy Library	1
Head of Aerospace and Mechanical Engineering, ADFA	1
Hargrave Library, Monash University	Doc Data Sheet
OTHER ORGANISATIONS	
National Library of Australia	1
NASA (Canberra)	1
INTERNATIONAL DEFENCE INFORMATION CENTRES	
US - Defense Technical Information Center	1
UK - Dstl Knowledge Services	1
Canada - Defence Research Directorate R&D Knowledge and Information Management (DRDKIM)	1

NZ - Defence Information Centre	1

ABSTRACTING AND INFORMATION ORGANISATIONS

Library, Chemical Abstracts Reference Service	1
Engineering Societies Library, US	1
Materials Information, Cambridge Scientific Abstracts, US	1
Documents Librarian, The Center for Research Libraries, US	1

SPARES

DSTO Edinburgh Library	5 (printed)

Total number of copies: printed 9, pdf 27

DEFENCE SCIENCE AND TECHNOLOGY ORGANISATION DOCUMENT CONTROL DATA	1. CAVEAT/PRIVACY MARKING

2. TITLE	3. SECURITY CLASSIFICATION
Tracking Anti-Ship Missiles Using Radar and Infra-Red Search and Track: Track Error Performance	Document (U) Title (U) Abstract (U)
4. AUTHORS	5. CORPORATE AUTHOR
Hwa-Tung Ong	Defence Science and Technology Organisation PO Box 1500 Edinburgh, South Australia 5111, Australia

6a. DSTO NUMBER	6b. AR NUMBER	6c. TYPE OF REPORT	7. DOCUMENT DATE
DSTO–TR–1863	013-655	Technical Report	June, 2006

8. FILE NUMBER	9. TASK NUMBER	10. SPONSOR	11. No OF PAGES	12. No OF REFS
2005/1054074/1	NAV 05/213	DGMD	18	11

13. URL OF ELECTRONIC VERSION	14. RELEASE AUTHORITY
http://www.dsto.defence.gov.au/corporate/reports/DSTO–TR–1863.pdf	Research Leader, Information Integration Branch

15. SECONDARY RELEASE STATEMENT OF THIS DOCUMENT

Approved For Public Release

OVERSEAS ENQUIRIES OUTSIDE STATED LIMITATIONS SHOULD BE REFERRED THROUGH DOCUMENT EXCHANGE, PO BOX 1500, EDINBURGH, SOUTH AUSTRALIA 5111

16. DELIBERATE ANNOUNCEMENT

No Limitations

17. CITATION IN OTHER DOCUMENTS

No Limitations

18. DSTO RESEARCH LIBRARY THESAURUS

Missile tracking
Infrared sensors
Data fusion
Antiship missiles
Radar tracking

19. ABSTRACT

The problem of association and fusion of radar and infra-red search and track (IRST) sensor reports is not straightforward, especially because IRST provides only angular measurements while radar provides range and range-rate measurements in addition to azimuth and elevation measurements. In this report, simulation results show that a centralised extended Kalman filter tracker is a solution that can capitalise on the higher angular accuracy of the IRST sensor to provide improved track accuracy performance.